Proc. Natl. Acad. Sci. USA
Vol. 96, pp. 5746–5751, May 1999
Neurobiology

Megacystis, mydriasis, and ion channel defect in mice lacking the α3 neuronal nicotinic acetylcholine receptor

WEI XU*†, SHARI GELBER‡, AVI ORR-URTREGER*§, DAWNA ARMSTRONG¶, RICHARD A. LEWIS*‖, CHING-NAN OU¶, JAMES PATRICK**, LORNA ROLE‡, MARIELLA DE BIASI††, AND ARTHUR L. BEAUDET*†‡‡

Departments of *Molecular and Human Genetics, ¶Pathology, ‖Ophthalmology, and ††Molecular Physiology and Biophysics, and **Division of Neuroscience, Baylor College of Medicine, and †Howard Hughes Medical Institute, Houston, TX 77030; and ‡Department of Anatomy and Cell Biology and Center for Neurobiology and Behavior, Columbia University College of Physicians and Surgeons, New York, NY 10032

Communicated by C. Thomas Caskey, Merck & Co., Inc., West Point, PA, march 23, 1999 (received for review December 15, 1998)

ABSTRACT **The α3 subunit of the neuronal nicotinic acetylcholine receptor is widely expressed in autonomic ganglia and in some parts of the brain. The α3 subunit can form heteromultimeric ion channels with other α subunits and with β2 and β4 subunits, but its function *in vivo* is poorly understood. We prepared a null mutation for the α3 gene by deletion of exon 5 and found that homozygous (−/−) mice lacked detectable mRNA on Northern blotting. The −/− mice survive to birth but have impaired growth and increased mortality before and after weaning. The −/− mice have extreme bladder enlargement, dribbling urination, bladder infection, urinary stones, and widely dilated ocular pupils that do not contract in response to light. Detailed histological studies of −/− mice revealed no significant abnormalities in brain or peripheral tissues except urinary bladder, where inflammation was prominent. Ganglion cells and axons were present in bladder and bowel. Bladder strips from −/− mice failed to contract in response to 0.1 mM nicotine, but did contract in response to electrical field stimulation or carbamoylcholine. The number of acetylcholine-activated single-channel currents was severely reduced in the neurons of superior cervical ganglia in −/− mice with five physiologically distinguishable nicotinic acetylcholine receptor subtypes with different conductance and kinetic properties in wild-type mice, all of which were reduced in −/− mice. The findings in the α3-null mice suggest that this subunit is an essential component of the nicotinic receptors mediating normal function of the autonomic nervous system. The phenotype in −/− mice may be similar to the rare human genetic disorder of megacystis–microcolon–intestinal hypoperistalsis syndrome.**

The neuronal nicotinic acetylcholine (ACh) receptor (nAChR) gene family consists of eight α subunits (α2–α9) and three β subunits (β2–β4), each containing four membrane-spanning domains (1–4). Expression studies in *Xenopus* oocytes have shown that any one of the α2, α3, or α4 subunits in combination with either β2 or β4 can produce functional receptors (2, 4–6). Diverse combinations of subunits occur, and even a single population of neurons can express multiple classes of nAChRs (7–9). The α3 subunit is widely expressed in autonomic ganglia and in some parts of the brain in multiple organisms (1, 2, 10–13). Although the role of α3-containing nAChRs in synaptic transmission in the central nervous system is not known, presynaptic receptors have been implicated in the modulation of the release of dopamine, norepinephrine, and glutamate (13–16).

In the peripheral autonomic nervous system, efferent signals are relayed by both sympathetic and parasympathetic ganglia. The α3 subunit is the predominant α gene expressed in these ganglia in the chicken (17). Functional deletion of the α3 subunit by antisense oligomers eliminated specific subtypes of channels expressed by chicken sympathetic neurons (8). In rat trigeminal sensory neurons, α3β4 is the principal subtype (18). The α3 subunit is expressed in all the parasympathetic neurons of rat intracardiac ganglia, which also express either or both the β2 and β4 subunits (12). Furthermore, transcripts encoding α3 are present in primate sympathetic ganglia (19). The consistent expression of α3 mRNA in the neurons of autonomic ganglia in different organisms suggests that the α3 subunit may be an important component of the nAChRs mediating fast synaptic transmission in the autonomic nervous system.

We have prepared a null mutation for the α3 subunit in mice, and we find that homozygous mice have megacystis with absence of bladder contraction in response to nicotine, widely dilated ocular pupils, and severely reduced ACh-activated single-channel currents in the neurons of superior cervical ganglia.

MATERIALS AND METHODS

Targeted Deletion of α3 Coding Gene. The murine α3 genomic locus was isolated from a mouse 129/SvEv genomic library (Stratagene) by using a rat cDNA clone for the α3 subunit (20). The intron/exon boundaries of exon 1 to exon 6 were determined by comparing the mouse genomic DNA sequence with the rat cDNA sequence (20). A detailed restriction map of the mouse α3 genomic locus is shown in Fig. 1*a*. The linearized targeting vector was electroporated into the AB2.1 embryonic stem (ES) cell line. After transformation, ES cell clones were grown on medium containing HAT (hypoxanthine, aminopterin, and thymidine) to select for cells expressing hypoxanthine phosphoribosyltransferase (HPRT), and 1-(2′-deoxy-2′-fluoro-β-D-arabinofuranosyl)-5-iodouracil (FIAU) was used for negative selection against the thymidine kinase (TK) gene. DNA from the selected clones was analyzed by Southern blotting with both 5′ and 3′ flanking probes, and one positive clone was expanded and injected into C57BL/6 blastocysts, as described (21). Male chimeras were bred to C57BL/6 females to produce the F_1 generation. The mutation in α3 was identified by Southern blot analysis and by three-way PCR with the primer sequences as follows: 5′-GTGGATCC-CTCCGGCCATCTTTAAGAG (wild-type forward), 5′-GA-CTGTGATGACAATGGACAAGGTGAC (wild-type reverse), and 5′-TGGCGCGAAGGGACCACCAAAGAA-CGG (mutant reverse). RNA blot analysis was employed to

The publication costs of this article were defrayed in part by page charge payment. This article must therefore be hereby marked "*advertisement*" in accordance with 18 U.S.C. §1734 solely to indicate this fact.

PNAS is available online at www.pnas.org.

Abbreviations: ACh, acetylcholine; nAChR, nicotinic acetylcholine receptor; CCH, carbamoylcholine; SCG, superior cervical ganglion.

§Present address: The Genetics Institute, Tel-Aviv Sourasky Medical Center, Tel-Aviv, Israel.

‡‡To whom reprint requests should be addressed at: Department of Molecular and Human Genetics, Baylor College of Medicine, Room T619, Houston, TX 77030. e-mail: abeaudet@bcm.tmc.edu.

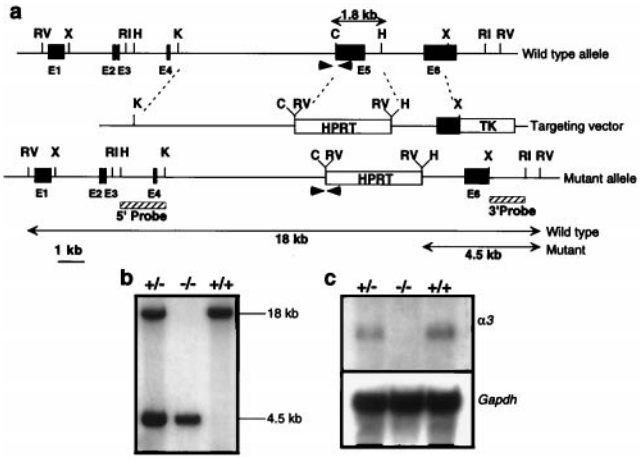

FIG. 1. Generation of α3-null mice. (*a*) Wild-type allele, targeting vector, and mutant allele are depicted with restriction enzyme sites, exons (solid rectangles), and 5′ and 3′ probes for Southern blotting. Restriction enzymes: RI, *Eco*RI; RV, *Eco*RV; C, *Cla*I; H, *Hin*dIII; K, *Kpn*I; and X, *Xho*I. TK, thymidine kinase; HPRT, hypoxanthine phosphoribosyltransferase. The 1.8-kb deleted region is indicated above the wild type allele. (*b*) Southern blot analysis of tail DNA from +/−, −/−, and +/+ littermates with the 3′ probe. (*c*) Northern blot analysis of expression of α3 in the brain of +/−, −/−, and +/+ littermates, using hybridization with a rat α3 cDNA (20) as a probe and a glyceraldehyde-3-phosphate dehydrogenase (*Gapdh*) probe as a control.

confirm that a null mutation had been generated in the α3 gene.

Histological, Morphological, and Physiological Analysis. The mice underwent complete gross autopsy. All organs were fixed in 10% formalin and sectioned at 5 μm. Sections were stained with hematoxylin/eosin and cresyl violet. Selected blocks of brain, bladder, and bowel were serially sectioned and variously stained with cresyl violet, or with immunohistochemistry, using the avidin-biotin techniques and the following antibodies: s100 (Z311), neuron-specific enolase (M873), and neurofilament protein (M762) from Dako and Map-2 (M4403; Boehringer Mannheim).

Blood was drawn from mice by retroorbital bleeding. To obtain urine samples from −/− mice and from other mice to test for bacterial infection, mice were sacrificed while they were under anesthesia and the abdomen was opened. Urine was immediately drawn from the bladder with a sterile syringe. A metabolic cage was used to collect urine from +/+ and −/− mice for urine chemistry studies. The composition of bladder stones was determined at the Mayo Medical Laboratories (Rochester, MN).

***In Vitro* Contractility Recording of Mouse Urinary Bladders.** Neonatal mice (2–4 days after birth) were decapitated. Urinary bladders were removed and placed into Krebs buffer aerated with a mixture of 5% CO_2/95% O_2. The Krebs solution had the following composition (mM): NaCl 119, KCl 4.7, KH_2PO_4 1.2, $NaHCO_3$ 25, $MgSO_4$ 1.5, D-glucose 11.0, and $CaCl_2$ 2.5. The bladders were opened longitudinally and cut into strips. After the urothelium had been gently removed, the strips were mounted vertically in organ baths filled with Krebs solution maintained at 37°C and aerated throughout the experiment. All smooth muscle preparations were stretched to a passive tension of 5 mN. The strips were allowed to equilibrate for about 1 hr with several changes of solution before exposure to electrical field stimulation (EFS) or drugs. Contractions were measured with an isometric transducer (Grass Instruments, Quincy, MA) and recorded on a chart recorder (Gould Instruments, Cleveland, OH). EFS was applied through a pair of platinum-wire electrodes lying in parallel to the smooth muscle strips. Frequency–response curves (1–35 Hz) were elicited by stimulating the tissues for 5 s with pulses of 5-ms duration at supramaximal voltage (50 V) every 60 s.

Nicotine was added as a single dose (0.1 mM) directly to the organ bath and was washed out after a maximum contraction was recorded. To determine relative response for each strip, a single dose of 0.1 mM carbamoylcholine (CCH) was added after a 1-hr interval with several changes of solutions. For dose responses to CCH, drug was added in cumulative doses from 10^{-7} M to 3×10^{-4} M after incubating the strips with 20 μM hexamethonium chloride for 20 min.

Preparation of Freshly Dispersed Neurons for Electrophysiological Recording. Freshly dispersed sympathetic neurons from mice were prepared from the superior cervical ganglia of mice at postnatal day 5–6. Ganglia were dissected into phosphate-buffered Ca^{2+}/Mg^{2+}-free saline and then desheathed and mechanically dispersed by repeated passage through a fire-polished Pasteur pipette in DMEM (GIBCO) supplemented with horse serum (10%), penicillin (50 units/ml), streptomycin (50 μg/ml), glutamine (2 mM), 2.5S nerve growth factor (Harlan Bioproducts for Science, Madison, WI), and DNase (2 mg/ml). The cells were plated on a 0.1% poly(L-ornithine) substrate. These freshly dispersed neurons were used for patch-clamp recording within 5–12 hr after plating.

Single-Channel Recordings. Single-channel recording utilized conventional cell-attached patch-clamp techniques (22) with extracellular recording solution consisting of 150 mM NaCl, 3 mM KCl, 2.5 mM $CaCl_2$, 3 μM tetrodotoxin, and 10 mM Hepes (titrated to pH 7.2 with 1 M NaOH). Neurons were visualized with phase-contrast optics at 400×. All experiments were done at room temperature.

Patch pipettes were pulled from Kimax capillary tubing (Kimble Glass, Vineland, NJ) on a vertical puller (Kopf, Tujunga, CA) and coated with Sigmacote (Sigma) to reduce capacitance. Signals were recorded with an Axopatch 200A patch-clamp amplifier (Axon Instruments, Foster City, CA). Pipettes contained 10 μM ACh dissolved in extracellular recording solution and their resistances were 4–5 MΩ.

The signal from the amplifier was stored for subsequent analysis with a VR-10B Digital Data Recorder (Instrutech, Great Neck, NY) and recorded on a Sony VCR. Data were filtered at 2–3 kHz (eight-pole low-pass Bessel filter; Frequency Devices, Haverhill, MA) and digitized with Fetchex (pClamp6 software, Axon Instruments). The single-channel records were analyzed by using Fetchan and pStat from pClamp6 to determine amplitude, frequency, and dwell time. Single-channel conductance was determined from the amplitude data by assuming a −50 mV resting potential. Statistical analysis and plot generation were performed using Microcal Origin 5.0 (Microcal Software, Northampton, MA), and τ values were determined by using a nonlinear curve-fitting subroutine with one or more summed Lorentzian distributions.

RESULTS

A null mutation in the α3 gene was produced in mouse embryonic stem (ES) cells by replacing a 1.8-kb region containing exon 5. This deletes three of the four transmembrane domains, the amphipathic helix domain implicated in channel formation, and the four cysteines essential for ligand binding (Fig. 1*a*). The mutation was transmitted to the germ line, and homozygous (−/−) mice lacked mRNA for α3 detectable on Northern blotting (Fig. 1 *b* and *c*).

No phenotypic abnormalities were noted in heterozygous (+/−) mice, and matings of heterozygotes produced −/− mice in the expected ratio of 25% at birth (27 −/−, 60 +/−, and 30 +/+ for litters shown in Fig. 2*a*). However, about 40% of −/− mice died from unknown causes in the first 3 days of life (Fig. 2*a*). Survival was then relatively stable until after weaning, and almost all remaining animals died over an

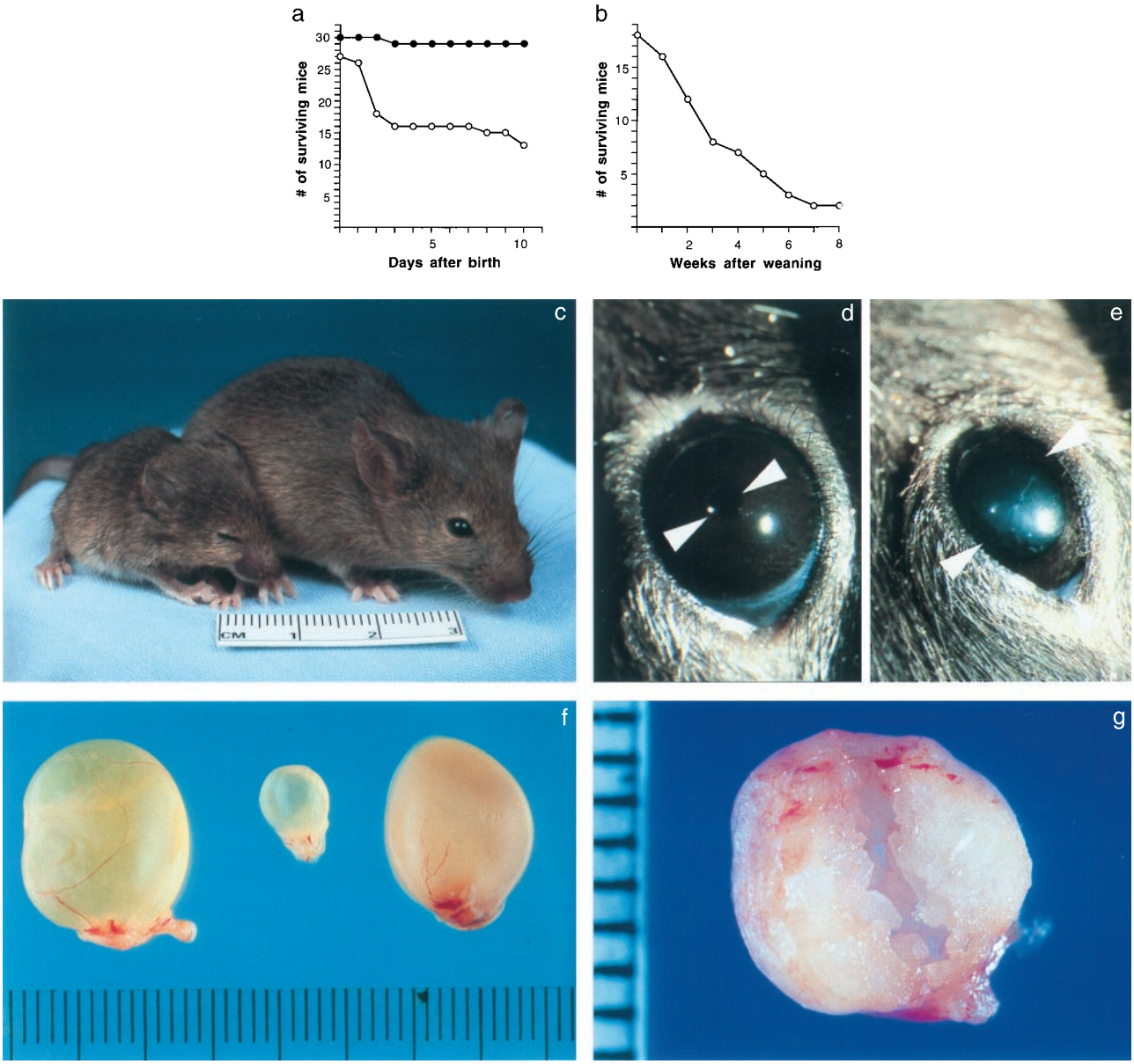

FIG. 2. Phenotypic findings in mice lacking the $\alpha 3$ nAChR subunit. Mice were bred on a mixed 129/SvEv and C57BL/6 background. (*a*) Survival of 27 $-/-$ (○) and 30 $+/+$ (●) littermate mice in the 10 days after birth. (*b*) Survival of 18 $-/-$ mice in the 8 weeks after weaning. (*c*) Comparison of typical $+/+$ (right) and $-/-$ (left) littermates at 7 weeks of age. Note smaller size and closed eyes in $-/-$ mouse. (*d* and *e*) Comparison of the eye in a $+/+$ mouse (*d*) demonstrating larger globe and tiny pupil compared with the smaller eye and very widely dilated pupil in the $-/-$ mouse (*e*). The margins of the pupils are indicated by white arrowheads. (*f*) The bladder from a normal mouse (center) is compared with two bladders from $-/-$ mice, the left containing clear urine and the right containing cloudy urine. (*g*) A $-/-$ mouse bladder that has been partially cut to demonstrate the dense stone formation filling the bladder.

interval of 6–8 weeks after weaning (Fig. 2*b*). All surviving mice were substantially growth impaired (Fig. 2*c*), with a mean weight approximately 40% of wild type at the time of weaning.

Careful examination of older mice revealed small palpebral fissures, smaller ocular globe perhaps in proportion to body size, and very widely dilated ocular pupils with no contraction in response to light (Fig. 2 *c–e*). In normal mice, the eyes are open by 2 weeks after birth, but in the $\alpha 3$ $-/-$ mice, the eyelids remain closed or nearly closed throughout life. The closed palpebral fissures may be related to dysfunction of the muscles opening the lids, the small size of the eye, or other developmental abnormality. Mydriasis and absence of pupillary constriction in response to light suggest that the autonomic input to the eyes is compromised in the $\alpha 3$ $-/-$ mice.

Gross anatomical dissection of animals dying spontaneously revealed severe distension of the urinary bladder in all cases, with the urine sometimes being clear and sometimes cloudy with dense accumulation of bacteria and white blood cells (Fig. 2*f*). Bacterial cultures of bladders with cloudy urine documented infection with organisms that included *Proteus vulgaris*, *Staphylococcus xylosus*, coagulase-negative *Staphylococcus*, *Staphylococcus aureus*, group D *Enterococcus* spp., and *Escherichia coli*. In animals dying at an older age, the bladder was most often packed with urinary stones (Fig. 2*g*). Bladder stones consisted of magnesium ammonium phosphate hexahydrate (struvite) and calcium phosphate (apatite) with different percentages of each component in individual mice; the percentage of struvite ranged from 10% to 100%. Careful examination of $-/-$ mice demonstrated wetness of the genital area with chronic urinary dribbling throughout life. Blood chemistries were measured, including glucose, electrolytes, phosphate, calcium, magnesium, urea nitrogen, creatinine, alanine

aminotransferase, aspartate aminotransferase, and bilirubin, and no consistent differences were observed between +/+ and −/− mice. Urine chemistries were measured, including glucose, electrolytes, phosphate, calcium, magnesium, and creatinine, and no consistent differences were found between +/+ and −/− mice. It is probable that the urinary tract dysfunction, bladder infection, and bladder stones contributed to the mortality of mice beyond weaning.

Detailed pathological and histological studies were performed on four −/− mice, two having died spontaneously and two being sacrificed. No lesions were identified in brain, heart, lungs, liver, pancreas, spleen, testes, adrenal glands, muscle, or salivary glands. In four −/− and seven +/+ mice, examination of the brain was performed on every third serial section. The spinal cord of three −/− and five +/+ mice was examined at three levels. No abnormalities of cortex, hippocampus, basal ganglia, brain stem, or spinal cord were detected with hematoxylin/eosin and Nissl stain, although this does not exclude functional abnormalities of the brain in these regions. The bladder was filled with stones in three of four mice examined. The bladder was distended in three mice and was inflamed and thick walled in one case. The bladder was inflamed in three of four −/− mice, and the mucosa was necrotic in three of four −/− mice. Sections of bladder and bowel were examined to identify ganglion cells and axons by using immunohistochemistry with antibodies to S100 protein, neuron-specific enolase, neurofilament, and Map-2, and ganglion cells were present in the −/− mice. Nerve fibers could be seen in all but the most necrotic regions of bladder. Bladder mucosa was dysplastic bordering on malignant in two of four −/− mice, and this lesion requires further study. The ureters were not dilated and the urethra was patent. Cortical cysts were seen in one kidney, and calcium deposition was found in the kidney in three of four −/− mice. The stomach and/or bowel was distended in three of four −/− mice, but the significance of this distention was not clear.

Because of the consistently distended bladders and dribbling urination, bladder strips were analyzed for contractility in response to nicotine and other agents. Bladder emptying is controlled primarily by the parasympathetic nervous system through the pelvic nerves (23). Signals are relayed from preganglionic to postganglionic neurons, and ACh released from postganglionic neurons elicits the contraction of bladder smooth muscles through the activation of muscarinic ACh receptors (23–25). To test whether lack of α3-containing nAChRs in pelvic ganglia might impair ganglionic transmission, we examined the contractility of bladder strips in response to 0.1 mM nicotine. Nicotine failed to elicit contraction with bladder strips from −/− mice, but substantial contraction occurred in +/+ and +/− littermates (Fig. 3 *a* and *b*). We used electrical field stimulation (EFS) to test whether neurotransmitter release from parasympathetic terminals was impaired in the α3 −/− mice. The frequency–response curves were superimposable for the α3 −/− and +/+ mice (Fig. 3*c*), suggesting that neurotransmitters can indeed be released from the parasympathetic nerve terminals through mechanisms alternative to neuronal stimulation. To further determine whether urinary dysfunction in α3 −/− mice is caused by a defect in smooth muscle contractility, we studied the responses to the muscarinic agonist CCH in the presence of the ganglionic blocker hexamethonium. CCH caused similar dose-dependent increase in contractility in α3 +/+ and −/− mice (Fig. 3*d*). Heterozygous mice were indistinguishable from +/+ mice in these bladder studies. These results suggest that smooth muscle responses in the −/− mice are normal and that bladder voiding is impaired because of the lack of expression of α3-containing nAChRs in neurons of pelvic ganglia.

In light of the defects in autonomic ganglionic transmission suggested by altered eye and bladder function observed *in vivo*, we assessed the profile of nicotinic elicited responses in

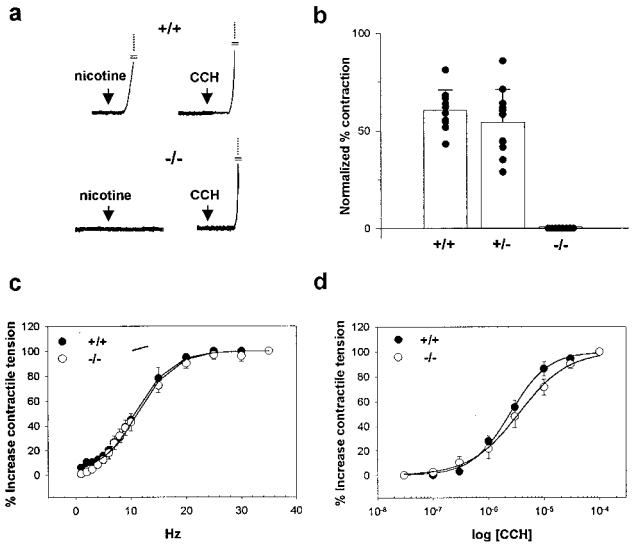

FIG. 3. Absence of bladder contraction in response to nicotine in α3-deficient mice. (*a*) Typical tracings of the response to nicotine and CCH in +/+ and −/− mice. (*b*) Response to nicotine in +/+ (n = 10), +/− (n = 11), and −/− (n = 8) mice. Data are presented as the contraction in response to nicotine as a percentage of that in response to CCH, ±SEM. (*c*) Bladder contraction in response to electric field simulation, showing indistinguishable response in +/+ and −/− mice. (*d*) Bladder contraction in response to CCH in +/+ and −/− mice, indicating comparable responses in the two groups.

ganglionic neurons directly by patch-clamp recording. The ACh receptor-elicited single-channel currents in peripheral autonomic nervous system were assessed in neurons of the superior cervical ganglion (SCG) from neonatal mice. This ganglion is accessible for study and contributes to sympathetic innervation of the eyelids (26), which may relate to the ocular phenotype in the mice. Comparison of −/− and +/+ mice indicated that α3 is required for expression of the full complement of ACh-activated channels normally detected in these neurons (Fig. 4). The representative recordings in Fig. 4*a* illustrate key features of ACh-elicited channels in +/+ and −/− SCG neurons. Currents were elicited by ACh in all patches from +/+ SCG neurons (n = 25 patches), whereas more than half of the patches from −/− SCG neurons were devoid of ACh-gated channels, assayed under identical conditions (n = 10 of 19 total patches; [ACh] = 10 μM; recording duration >10 min); robust K^+ channel activity was recorded in all patches lacking detectable ACh-gated events. Analysis of the ACh-gated channels recorded in nine patches from +/+ SCG neurons yielded a high nAChR opening probability and high event frequency (P_O = 0.15 ± 0.19; range 0.027–0.346). The frequency range was 1.2–12 events per s; 9×10^3 events per 45 min. As shown in Fig. 4*b*, the +/+ SCG neurons typically expressed five physiologically distinguishable nAChR "subtypes" with different conductance and kinetic properties ($\gamma 1_{+/+} \approx 9$ pS; $\gamma 2_{+/+} \approx 18$ pS; $\gamma 3_{+/+} \approx 25$ pS; $\gamma 4_{+/+} \approx 35$ pS; and $\gamma 5_{+/+} \approx 41$ pS).

Analysis of the nine patches from −/− SCG neurons in which some ACh-gated channel activity was detected revealed significantly lower P_O and opening frequency (P_O = 0.009 ± 0.01; range 0.001–0.037). The frequency range was 0.024–1.2 events per s; 2×10^3 events per 45 min. In addition, there were fewer discernable γ classes ($\gamma 1_{-/-} \approx 18$ pS and $\gamma 2_{-/-} \approx 25$ pS) than in neurons from +/+ littermates. Analysis of the nAChR channel kinetics revealed that the −/− 18-pS and 25-pS events were uniformly brief in opening duration, whereas in +/+ neurons, both of these subtypes include three kinetic components. The similarity in the fastest component of the −/− and +/+ 18-pS and 25-pS subtypes suggests that these rapid events

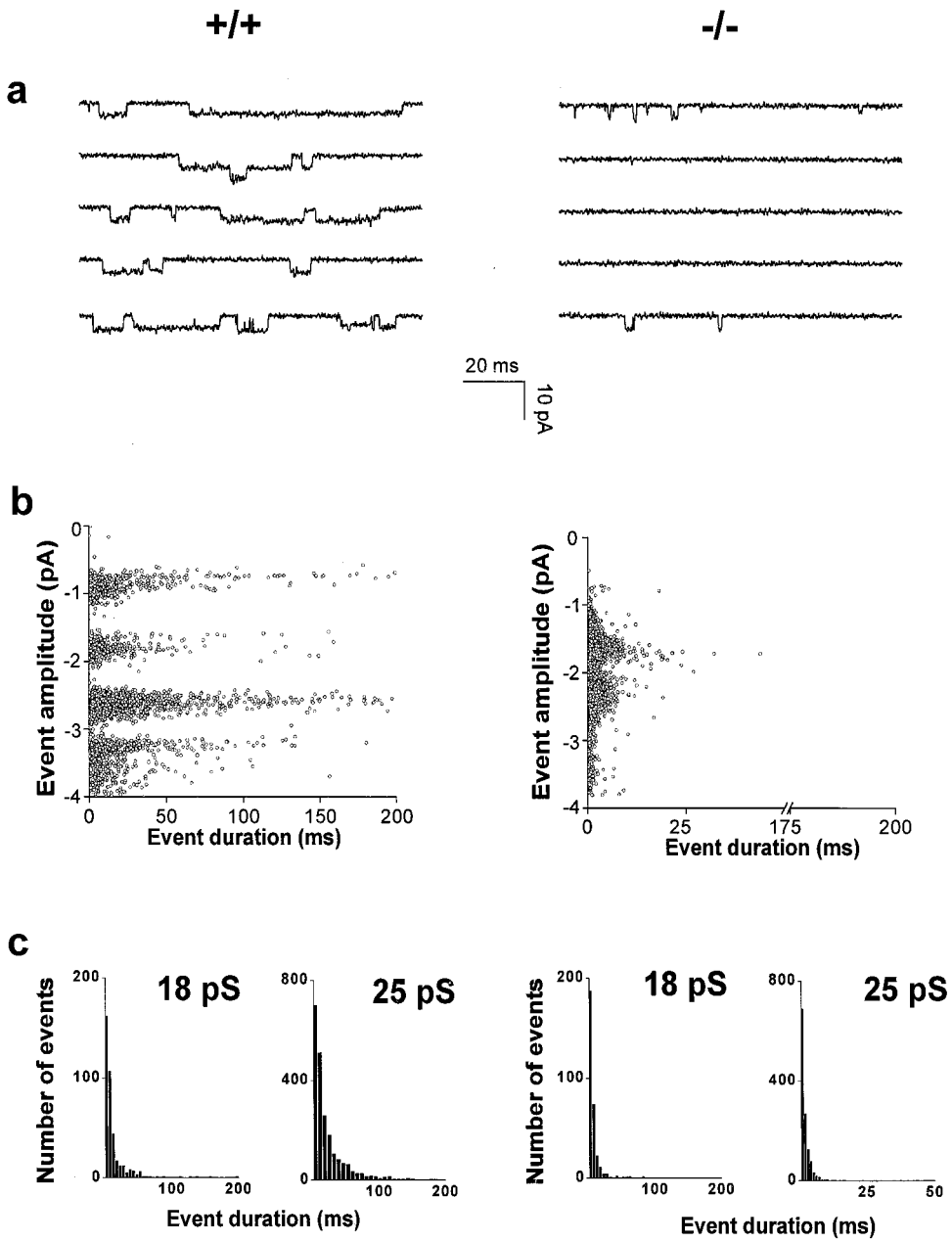

FIG. 4. Altered profile of ACh-elicited single-channel currents in SCG neurons in α3-deficient mice. The SCG neurons from +/+ mice express five conductance classes of nAChRs. In contrast, the SCG neurons from −/− mice display many fewer channel openings which contribute to only two well-defined conductance classes. (*a*) Sample traces of ACh-gated single-channel currents in cell attached patches (membrane holding potential +50 mV) demonstrated that the +/+ mice expressed both more channel openings and openings of longer duration than the −/− mice. (*b*) Amplitude analysis of +/+ SCG neurons indicated that there were five amplitude classes ($\gamma 1_{+/+} \approx 9$ pS, $\gamma 2_{+/+} \approx 18$ pS, $\gamma 3_{+/+} \approx 25$ pS, $\gamma 4_{+/+} \approx 35$ pS, and $\gamma 5_{+/+} \approx 41$ pS; 3,148 events pooled from four cells). In contrast, amplitude analysis of −/− SCG neurons revealed only two well defined conductance classes ($\gamma 1_{-/-} \approx 18$ pS and $\gamma 2_{-/-} \approx 25$ pS; 2,185 events pooled from nine cells). (*c*) Kinetic analysis of the 18-pS and 25-pS channel classes from both +/+ and −/− mice showed that the fast components of both classes were similar in the +/+ and −/− mice. However, the +/+ channels each contained two longer-duration components that were missing from the −/− classes. Mean τ values ± SEM are reported in the text.

may not normally include α3. Mean τ values ± SEM in ms were determined as described in *Materials and Methods* (for +/+ 18-pS: $\tau_1 = 3.8 \pm 0.03$, $\tau_2 = 9.8 \pm 0.13$, $\tau_3 = 26.5 \pm 3.37$; for +/+ 25-pS: $\tau_1 = 3.2 \pm 0.09$, $\tau_2 = 8.2 \pm 0.59$, $\tau_3 = 21.1 \pm 5.91$; for −/− 18-pS: $\tau_0 = 4.4 \pm 0.10$; for −/− 25-pS: $\tau_0 = 2.5 \pm 0.03$). The lack of correspondence of the conductance and kinetic properties of the +/+ nAChR channels with the majority of those detected in −/− neurons suggests that deletion of α3 blocks the expression of the five channel subtypes observed in +/+ mice. Data were not collected from +/− mice.

The simplest interpretation of these studies is that the α3 subunit normally participates in the majority of +/+ nAChR channels expressed in the SCG; therefore its absence results in the loss of most nAChR channels in SCG neurons. Alternatively, the deletion of α3 may influence the synthesis and/or assembly of nAChR channels, thereby interfering with the assembly or localization of the usual array of nAChR complexes whether or not they include α3. Consistent with a role in localization, α3 was recently reported to be essential for targeting α3-containing nAChRs to the interneuronal synapse *in vivo* in the chicken ciliary ganglion (27). Finally it is

interesting to note that recordings from $-/-$ neurons with detectable nAChR activity often included ACh-gated events that were biophysically distinct from any of the nAChR channels detected in $+/+$ neurons (i.e., "mutant" nAChRs are present in $-/-$ neurons). The expression of these aberrant nAChR channels is reminiscent of results obtained in studies of neurons treated with antisense oligonucleotides targeted against the α3 subunit (8).

DISCUSSION

The major phenotypic findings in mice deficient for the α3 nAChR include unexplained lethality in the first week of life, postnatal growth deficiency, megacystis, and mydriasis. The data are most consistent with a severe reduction or absence of contractility of the bladder as the cause of the megacystis with secondary dribbling urination, urinary retention, bladder infection, and bladder stone formation. Considering the known physiology of micturition, the expression pattern for α3, and—by analogy—the deficit in nAChR-elicited currents in the SCG, the lack of bladder contractility is likely to be caused by the absence of α3-containing nAChRs in the parasympathetic intramural ganglia of the bladder. A deficit of fast-synaptic transmission within these ganglia would explain the lack of innervation-dependent signaling for bladder contraction, and it would be consistent with the localization of α3 complexes to the interneuronal synapse (27). Because the micturition reflex has both peripheral and central components, we cannot exclude the possibility that deficiency of α3 may also affect areas such as the pontine-mesencephalic micturition center (28). The mortality that occurs after weaning may be related to bladder dysfunction and urinary tract infection.

Extreme mydriasis with absence of contraction in response to light is another prominent phenotypic feature in the α3-deficient mice and is accompanied by failure to open the palpebral fissures and smaller size of the ocular globe. The decreased size of the eye may be a nonspecific aspect of the overall growth failure, and failure to open the eyes may represent palpebral ptosis and/or some developmental abnormality. The most definitive ocular finding is the extreme mydriasis with absence of contracture in response to light, and this likely reflects altered innervation of the ciliary body that controls contraction and dilatation of the pupil. On the basis of the known physiology, the expression pattern for α3, and single-channel recordings from the SCG, the data would be most consistent with impaired parasympathetic input leading to mydriasis.

The phenotype in the α3-deficient mice may be analogous to the human condition of megacystis–microcolon–intestinal hypoperistalsis syndrome (MMIHS). MMIHS is an autosomal recessive condition, and a review of 43 cases in 1991 (29) reported the following: normal birth weight, mean survival of 3.6 months, megacystis in 100%, hydronephrosis/hydroureter in 88%, microcolon in 91%, intestinal hypoperistalsis in 100%, and normal abundance of ganglion cells in the intestine in 100% of cases. Mydriasis was not reported, and the disorder is essentially lethal despite attempts at surgical and pharmacologic intervention. On the basis of phenotypic similarity, it would be of interest to search for mutations in the α3 subunit of nAChR in this human syndrome. Similarly, it would be of interest to investigate intestinal peristalsis in the α3-deficient mice. It is possible that dysfunction of the autonomic nervous system in the α3-deficient mice is considerably more extensive than currently documented. Effects on cardiac function also should be evaluated.

In conclusion, genetic analysis of the function of the α3 subunit indicates that it is essential for autonomic control of some peripheral organs, with the most obvious phenotypic effects on survival, growth, bladder function, and pupillary contraction. The results indicate that functional redundancy is not extensive for α3 despite the coexpression of other subunits, including α5 and α7, in many α3-expressing structures. The α3-deficient mice are too ill for meaningful behavioral studies, and no phenotypic features clearly attributable to central nervous system (CNS) dysfunction were readily identified; a conditional mutation limited to the CNS would be useful for evaluating the function of α3 in central tissues.

We thank Isabel Lorenzo, Barbara Antalffy, and Garland Cantrell for technical assistance and Naveen Agnihotri for computer programming. R.A.L. is a Senior Research Scientist with Research to Prevent Blindness. This work was supported by National Institutes of Health Grants DA-09366 to L.W.R. and NS-13546 and DA-04077 to J.P. and through Mental Retardation Research Center Grant HD-24064.

1. Sargent, P. B. (1993) *Annu. Rev. Neurosci.* **16,** 403–443.
2. McGehee, D. S. & Role, L. W. (1995) *Annu. Rev. Physiol.* **57,** 521–546.
3. Le Novere, N. & Changeux, J.-P. (1995) *J. Mol. Evol.* **40,** 155–172.
4. Colquhoun, L. M. & Patrick, J. W. (1997) *J. Neurochem.* **69,** 2355–2362.
5. Lindstrom, J., Anand, R., Gerzanich, V., Peng, X., Wang, F. & Wells, G. (1996) *Prog. Brain Res.* **109,** 125–137.
6. Patrick, J., Sequela, P., Vernino, S., Amador, M., Leutje, C. & Dani, J. A. (1993) *Prog. Brain Res.* **98,** 113–120.
7. Conroy, W. G., Vernallis, A. B. & Berg, D. K. (1992) *Neuron* **9,** 679–691.
8. Listerud, M., Brussaard, A. B., Devay, P., Colman, D. R. & Role, L. W. (1991) *Science* **254,** 1518–1521.
9. Goldman, D., Deneris, E., Luyten, W., Kochhar, A., Patrick, J. & Heinemann, S. (1987) *Cell* **48,** 965–973.
10. Wada, E., Wada, K., Boulter, J., Deneris, E., Heinemann, S., Patrick, J. & Swanson, L. W. (1989) *J. Comp. Neurol.* **284,** 314–335.
11. Rust, G., Burgunder, J.-M., Lauterburg, T. E. & Cachelin, A. B. (1994) *Eur. J. Neurosci.* **6,** 478–485.
12. Poth, K., Nutter, T. J., Cuevas, J., Parker, M. J., Adams, D. J. & Luetje, C. W. (1997) *J. Neurosci.* **17,** 586–596.
13. Wonnacott, S. (1997) *Trends Neurosci.* **20,** 92–98.
14. Sacaan, A. I., Dunlop, J. L. & Lloyd, G. K. (1995) *J. Pharmacol. Exp. Ther.* **274,** 224–230.
15. Pidoplichko, V. I., De Biasi, M., Williams, J. T. & Dani, J. A. (1997) *Nature (London)* **390,** 401–404.
16. McGehee, D. S., Heath, M. J. S., Gelber, S., Devay, P. & Role, L. W. (1995) *Science* **269,** 1692–1696.
17. Role, L. W. & Berg, D. K. (1996) *Neuron* **16,** 1077–1085.
18. Flores, C. M., DeCamp, R. M., Kilo, S., Rogers, S. W. & Hargreaves, J. M. (1996) *J. Neurosci.* **16,** 7892–7901.
19. Cimino, M., Marini, P., Fornasari, D., Cattabeni, F. & Clementi, F. (1992) *Neuroscience* **51,** 77–86.
20. Boulter, J., Evans, K., Goldman, D., Martin, G., Treco, D., Heinemann, S. & Patrick, J. (1986) *Nature (London)* **319,** 368–374.
21. Bradley, A. (1987) *Teratocarcinomas and Embryonic Stem Cells; A Practical Approach* (IRL, Oxford).
22. Hamill, O. P., Marty, A., Neher, E., Sakmann, B. & Sigworth, F. J. (1981) *Pflügers Arch.* **391,** 85–100.
23. Wein, A. J. & Barrett, D. M. (1988) *Voiding Function and Dysfunction: A Logical and Practical Approach* (Year Book Medical, Chicago).
24. Levin, R. M., Shofer, F. S. & Wein, A. J. (1980) *J. Pharmacol. Exp. Ther.* **212,** 536–540.
25. Wang, P., Luthin, G. R. & Ruggieri, M. R. (1994) *J. Pharmacol. Exp. Ther.* **273,** 959–966.
26. Large, B. J. (1975) *Br. J. Pharmacol.* **54,** 351–358.
27. Williams, B. M., Temburni, M. K., Levey, M. S., Bertrand, S., Bertrand, D. & Jacob, M. H. (1998) *Nat. Neurosci.* **1,** 557–562.
28. Nishizawa, O., Sugaya, K. & Shimoda, N. (1998) *Scand. J. Urol. Nephrol. Suppl.* **175,** 15–19.
29. Anneren, G., Meurling, S. & Olsen, L. (1991) *Am. J. Med. Genet.* **41,** 251–254.